Supporting Information

Figure S1 a

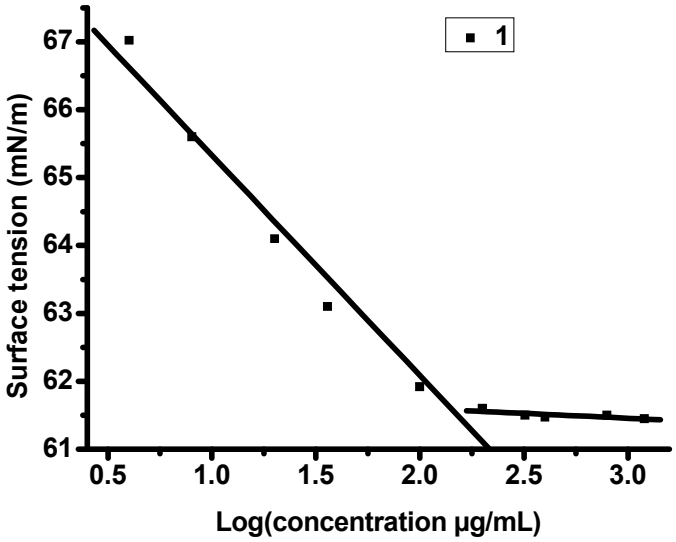

Figure S1 b

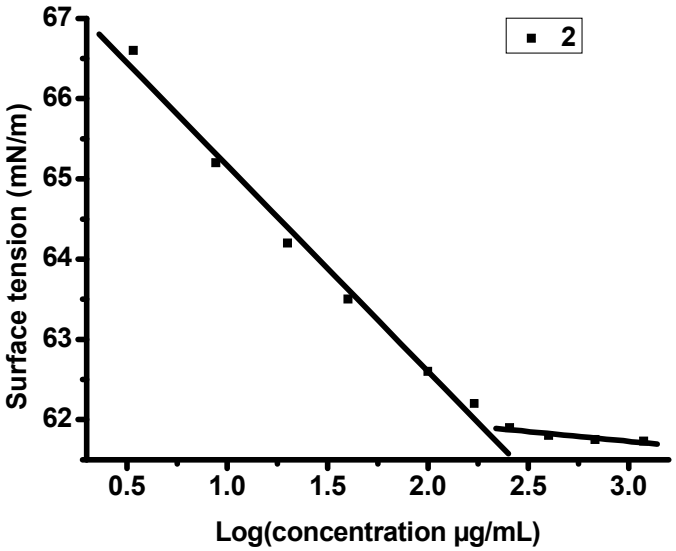

Figure S1 c

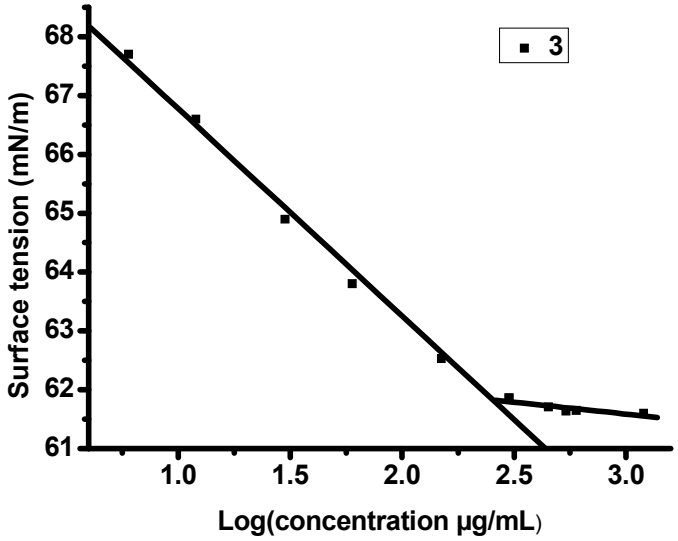

Solutions of **1**, **2** and **3** in water were made at the concentrations indicated in the figure. The vials were agitated gently overnight to promote the formation of micelles. The surface tension (mN/m) was measured for each solution. The surface tensions determined were plotted against the log of the concentration of **1, 2** and **3**. The inflection point as determined by the best fit of the data yielded CMC's of 0.18 mg/mL for **1**, 0.2 mg/mL for **2** and 0.25 mg/mL for **3**.

Figure S2

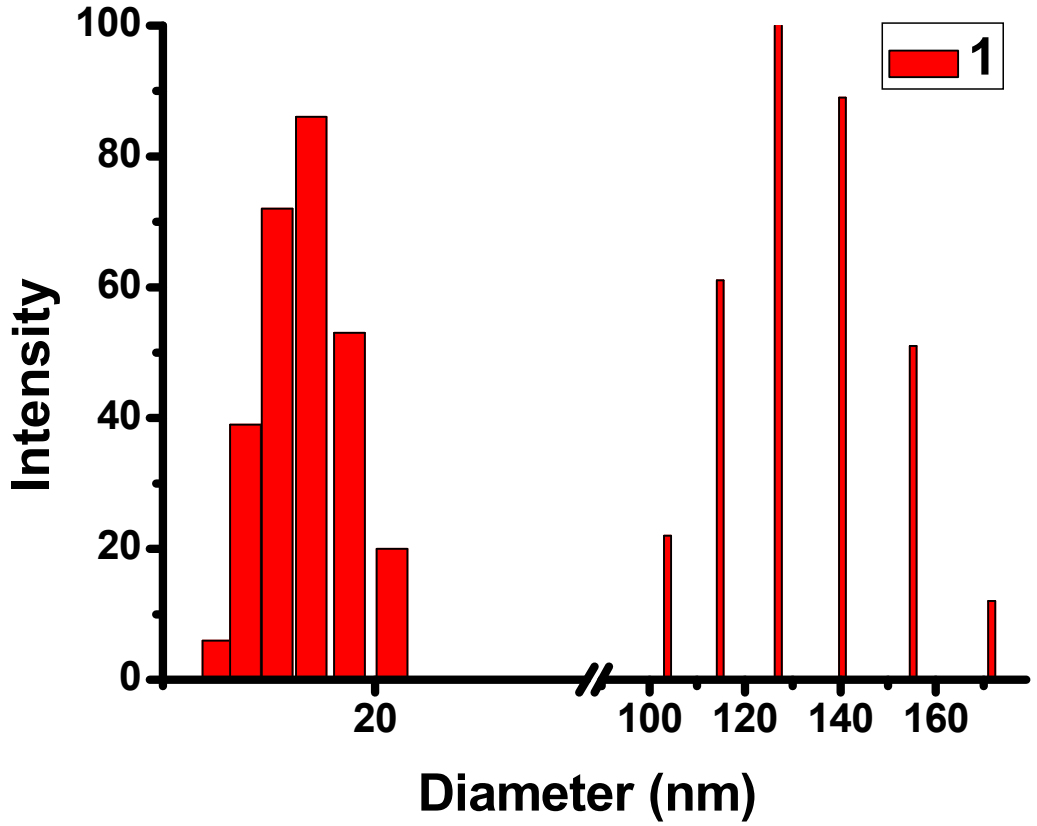

Dynamic Light Scattering of 1 mg/mL of **1** in water shows hydrated monomer scattering at 16.7 nm with an average polydispersity of 0.095 and micelles with mean diameter of 132.7 nm with an average polydispersity of 0.12.

Figure S3

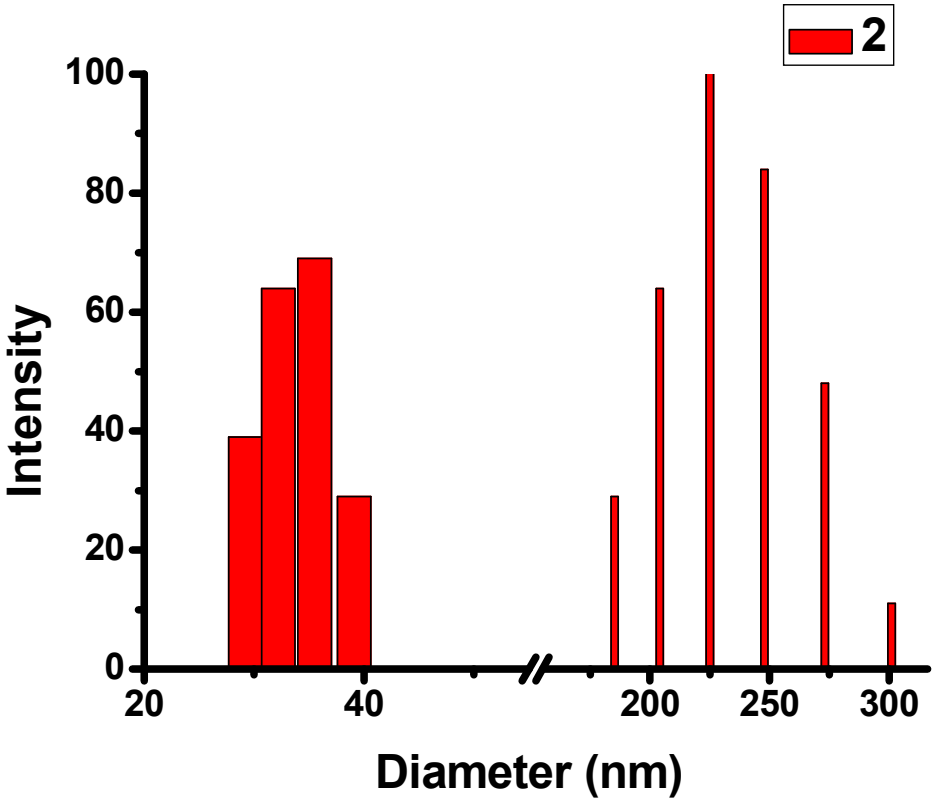

Dynamic Light Scattering of 1 mg/mL of **2** in water shows hydrated monomer scattering at 33.7 nm in diameter with an average polydispersity of 0.08 and micelle of mean diameter 232.6 nm with an average polydispersity of 0.12.

Figure S4

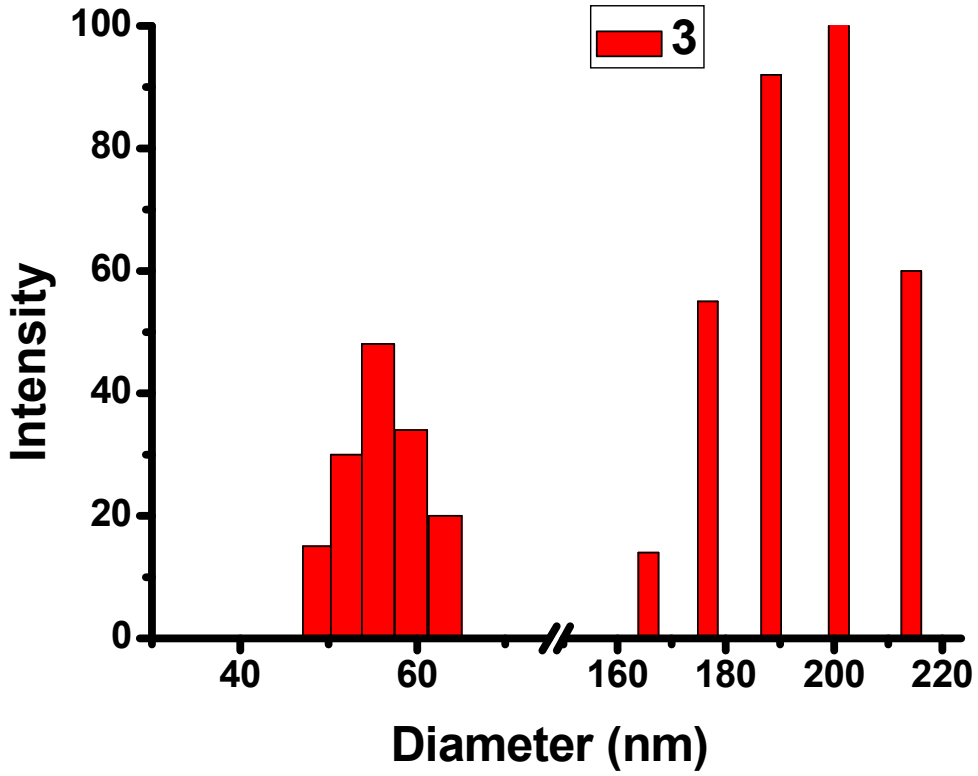

Dynamic Light Scattering of 1 mg/mL of **3** in water shows hydrated monomer scattering of 56.1 nm in diameter with an average polydispersity of 0.08 and mean micelle diameter of 196.3 nm with an average polydispersity of 0.09.

Figure S5

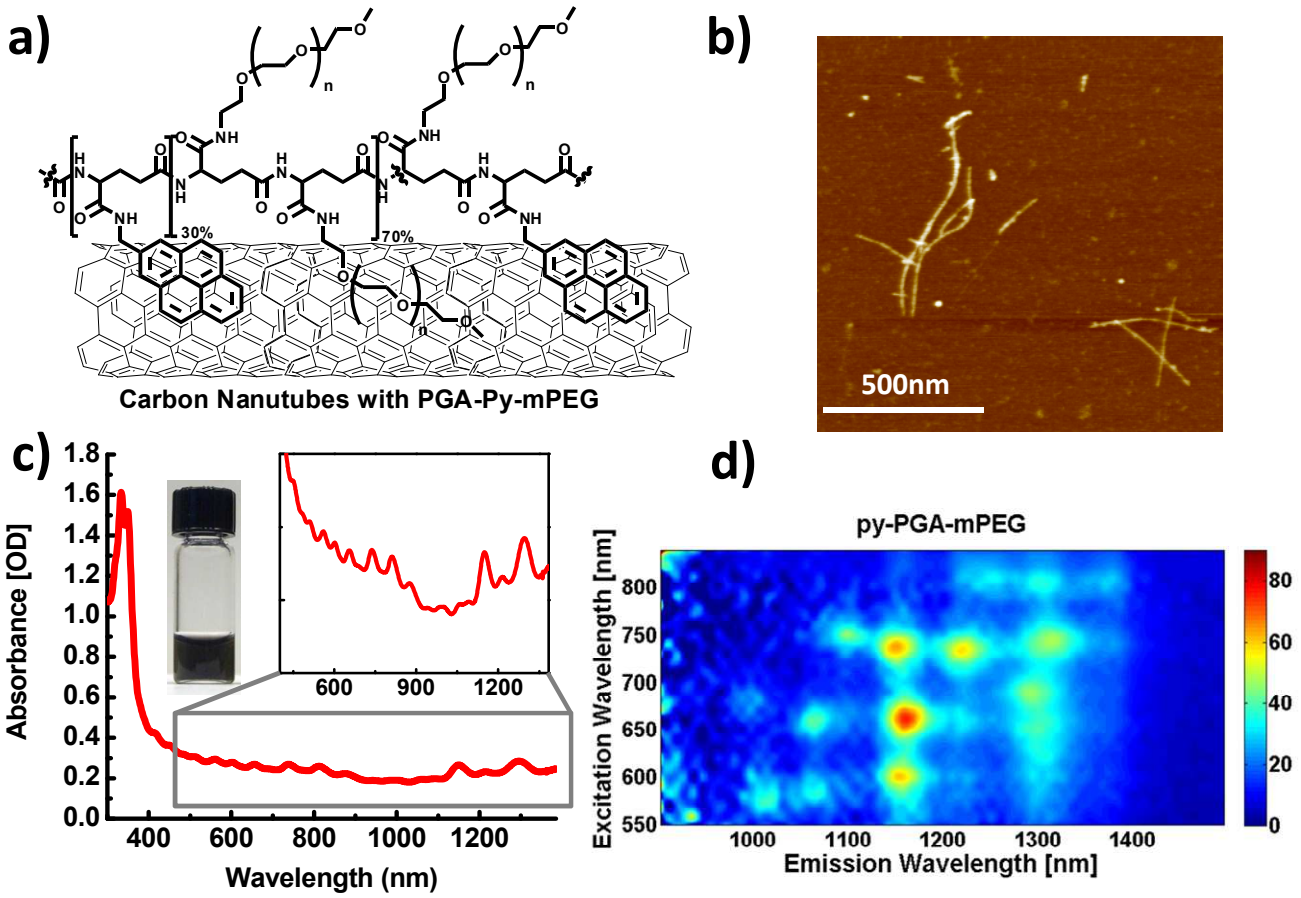

a) Single walled carbon nanotubes (SWNTs) coating with (**2**). b) AFM image of SWNTs with (**2**) coating. Non-uniform height along the nanotube is attributed to presence of the polymer coating. c) The UV-Vis-NIR absorption spectrum of SWNTs with (**2**) coating with excess polymer remove. Inset: solution photo. Spectrum shows large pyrene absorption below 400nm, indicating its binding to the SWNTs. d) Photoluminescence versus excitation (PLE) spectrum of SWNTs with (**2**) coating. Horizontal axis shows photoluminescence spectrum at different excitations along the vertical axis. Bright spots correspond to SWNTs of different chiralities, demonstrating that the inherent NIR photoluminescent properties are not lost with the (**2**) coating.

Figure S6

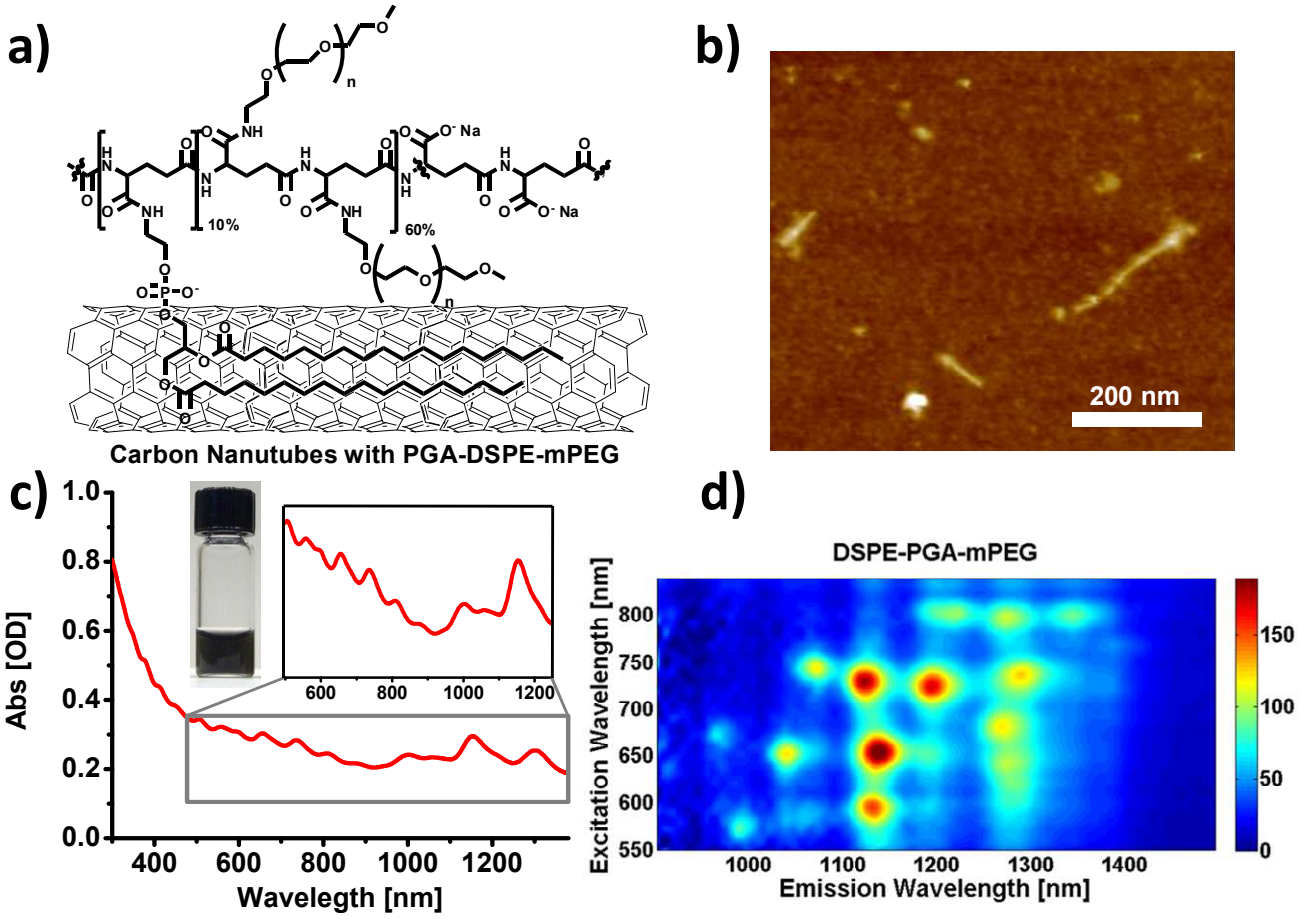

a) Single walled carbon nanotubes (SWNTs) coating with (**3**). b) AFM image of SWNTs with (**3**) coating. Non-uniform height along the nanotube is attributed to presence of the polymer coating. c) The UV-Vis-NIR absorption spectrum of SWNTs with (**3**) coating with excess polymer remove. Inset: solution photo. d) Photoluminescence versus excitation (PLE) spectrum of SWNTs with (**3**) coating. Horizontal axis shows photoluminescence spectrum at different excitations along the vertical axis. Bright spots correspond to SWNTs of different chiralities, demonstrating that the inherent NIR photoluminescent properties are not lost with the (**3**) coating.

Figure S7

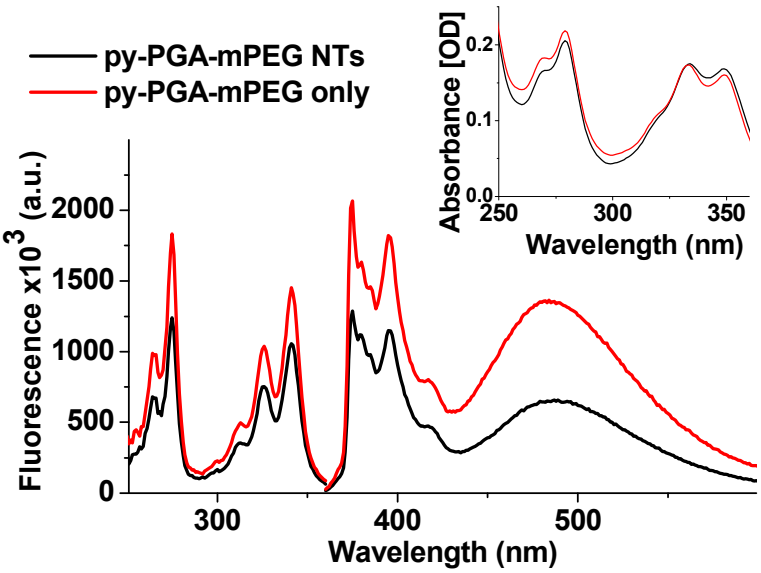

While $PMHC_{18}$ likely interacts with the SWNT sidewall via van der Waals' and entropic forces, the pyrene moiety has been reported to demonstrate a strong tendency to adsorb on SWNTs by π-stacking and hydrophobic interactions in aqueous media[2- 5, 6].Proof of the intimate interaction between pyrene and the NT sidewall was observed by quenching of pyrene fluorescence relative to free pyrene-containing methoxyPEG-γPGA at the same OD.

Figure S8

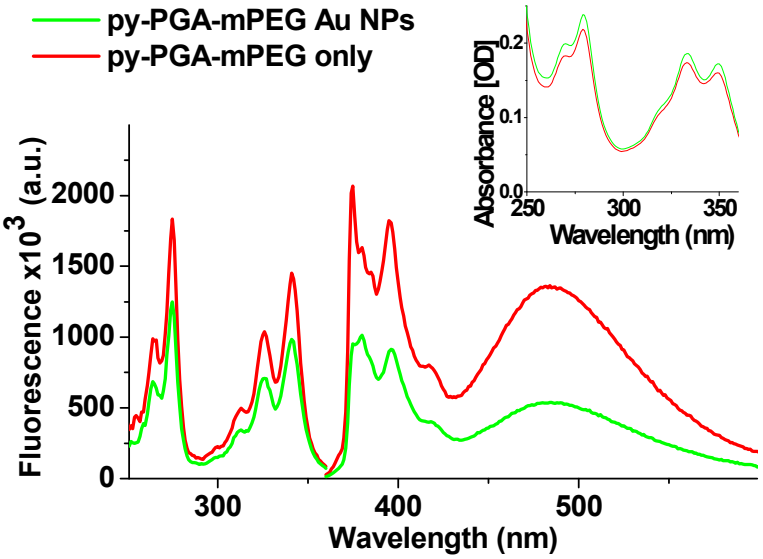

The intensity of pyrene adsorbance is dampened due to perturbations of gold nanoparticles, suggesting direct interaction of pyrene with the gold surface[5, 7].

Figure S9

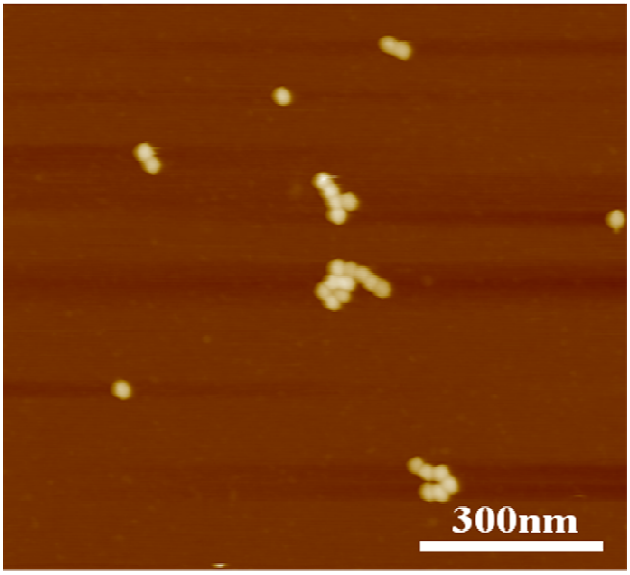

AFM image of gold NPs with thiol-mPEG (5KDa) after removing excess PEG. Individualized NPs are stable only in the presence of excess thiol-mPEG, and indeed, if the excess of the thiol-mPEG is removed by centrifugation, the solution of NPs become unstable, forming aggregates.

Methods

General Materials and Methods. UV-visible spectra were recorded using a Varian Cary 300 UV-visible spectrophotometer. ^{1}H NMR spectra were recorded on a Varian 500 MHz instrument as dilute solutions, 15 Hz sample spin and 60º pulse angle, in deuterated water and CCl_3D, with delay times of 12 and 8 seconds respectively. The chemical shifts are reported relative to tetramethylsilane. AFM (atomic force microscopy) images were recorded on a Veeco Nanosage IIIa. The TEM (transmission electron microscopy) images were recorded with Philips CM20 FEG-TEM. Dynamic Light Scattering measurements were obtained on a Brookhaven Instruments 90Plus Particle Size Analyzer. The CMC (critical micelle concentration) was recorded with KSV Minimicro Langmuir-Blodgett System 2 instrument at r.t. Photoluminescence excitation (PLE) measurements in the NIR

were performed utilizing a home-built setup. A short arc lamp (Osram XBO 75W/2 OFR 75W Xenon lamp installed into Oriel 66907 Arc Lamp Source) and a monochromator (Oriel 7400 Cornerstone 130 monochromator) were used to supply excitation light in the 550 nm – 840 nm range in 10 nm steps. The excitation light was focused onto a sample placed in a 1 mm path quartz cuvette. The room temperature photoluminescence was collected at the opposite cuvette wall and the PL spectrum was recorded using a second monochromator (Acton SpectraPro 2300i) and a liquid nitrogen-cooled InGaAs array detector (Princeton Instruments OMA V 1024-2.2 LN) in the 900–1500 nm range. As-obtained PL spectra were scaled by the measured excitation power (measured using Oriel 71580 calibrated Si photodiode) before obtaining a PLE spectrum by interpolating the thirty measured PL spectra. The bandpass used for emission and excitation was 15nm.

Dialysis membranes of regenerated cellulose were purchased from Ficher Scientific with 12,000-14,000 MWCO. For vacuum filtration, isopore membrane filters of 0.2 μm were purchased from Millipore.

Single-walled carbon nanotubes (SWNTs) were obtained from Carbon Nanotechnologies Incorporated and used without further purification. Gold colloid nanoparticles of average diameter 20 nm were obtained from Sigma-Aldrich, as 0.7-0.9% solid material basis, 0.01% $HAuCl_4$ and used as received. The poly-(γ-glutamic acid) γPGA was obtained from Natto Bioscences with an average molecular weight of ~ 430 KDa. 1-pyrenemethylamine hydrochloride was obtained from Sigma-Aldrich. The Poly(maleic anhydride-alt-1-octadecene) was obtained from Sigma-Aldrich with a molecular weight of 30,000-50,000 Da. The poly(ethylene glycol) methyl ether (mPEG-NH_2, MW 5000 Da) was obtained from Laysan Bio, Inc.

Synthesis of $PMHC_{18}$-mPEG(100%, 5KDa) (1). Poly(maleic anhydride-alt-1-octadecene) (10 mg, 0.0286 mmol) was reacted with poly(ethylene glycol) methyl ether (285.7 mg, 0.05714 mmol, mPEG-NH_2, 5 KDa) in 15 mL DMSO/Pyridine 9/1. After 12 h it was added the 1-ethyl-3-(3-dimethylaminopropyl)carbodiimide hydrochloride (21.8 mg, 0.11 mmol) (EDC.HCl). After another 24 h reaction the resulting polymer was purified to remove byproduct by dialysis with 12,000-14,000 MWCO with distilled water. The solvent was removed by lyophilization to yield 240 mg of (**1**) yellow/white solid (yield ~81%).

The average number of PEG groups bound to $PMHC_{18}$ chains was determined by ^{1}H NMR in $CDCl_3$, comparing the integrated signal at 3.7-3.4 ppm (broad, CH_2 of PEG) with that at 1.0-1.3 ppm (CH_2 of C_{18} chains). The effective degree of modification was found to be 2 molecules of mPEG for each unit of $PMHC_{18}$. ^{1}H NMR (500 MHz, $CDCl_3$) δ: 3.7-3.4 (m, br, CH_2 of mPEG), 1.3-1.0 (m, CH_2 PMHC18), 0.88 ppm (m, br, CH_3 of $PMHC_{18}$).

Synthesis of PGA-Py(30%)-COOH. γPGA (100 mg, 0.66 mmol) was reacted with 1-pyrenemethylamine hydrochloride (61.4 mg, 0.23 mmol) in the presence of 1-ethyl-3-(3-dimethylaminopropyl)carbodiimide hydrochloride (EDC.HCl) (171.0 mg, 0.66 mmol) in 10 ml of 8/1/1 DMSO/Pyridine/Water. After 24 h reaction the resulting polymer was dialyzed against distilled water in a 12,000-14,000 MWCO regenerated cellulose dialysis tube. The solvent was removed by lyophilization to yield 120 mg of yellow solid (yield ~87%).

The average number of pyrene groups bound to PGA chains was determined by ^{1}H NMR in D_2O, comparing the integrated signal at 6.8-7.2 ppm (broad, 9 aromatic CH of pyrene) with that at 3.9 ppm (CH of glutamic acid). The effective degree of modification was found to be 30%. ^{1}H NMR (500

MHz, D_2O) δ: 6.8-7.2 (m, br, pyrene), 4.2 (m, br, CH_2-Pyrene), 3.9 (m, 1H, $NHCH_2$), 2.2 (m, 2H, CH_2 of PGA), 1.9-1.7 (m, 2H, CH_2 of PGA).

Synthesis of PGA-Py(30%)-mPEG(70%, 5KDa) (2). Pyrene-γPGA (30% Pyrene) (10 mg, 0.047 mmol) was reacted with poly(ethylene glycol) methyl ether (230 mg, 0.046 mmol, mPEG-NH_2, 5KDa) in the presence of 1-ethyl-3-(3-dimethylaminopropyl)carbodiimide hydrochloride (19.2 mg, 0.1 mmol) (EDC.HCl) in 15mL DMSO/Pyridine 9:1. After 24 h reaction the resulting polymer was purified to remove byproduct by dialysis with 12,000-14,000 MWCO with distilled water. The solvent was removed by lyophilization to yield 180 mg of (**2**) yellow/white solid (yield ~75%).

Estimation of PEG and pyrene groups were determined by ^{1}H NMR in D_2O, comparing the integrated signal at 7.2-6.8 (CH of pyrene) and at 3.4-4.0 ppm (CH_2 of PEG) with that at 2.6-1.8 ppm (CH_2 of PGA). The effective degree of modification was found to be 30 % of pyrene and 65-70% of mPEG. ^{1}H NMR (500 MHz, $CDCl_3$) δ: 7.2-6.8 (m, br, pyrene), 4.2-3.9 (m, br, CH_2-Pyrene, CH PGA), 3.8-3.4 (m, br, CH_2-mPEG), 2.6-1.8 (m, $2CH_2$ PGA).

Synthesis of PGA-mPEG(60%, 5KDa)-COOH. γPGA (10 mg, 0.066 mmol) was reacted with poly(ethylene glycol) methyl ether (200 mg, 0.040 mmol, mPEG-NH_2, MW 5000) in the presence of 1-ethyl-3-(3-dimethylaminopropyl)carbodiimide hydrochloride (EDC.HCl) (68.7 mg, 0.36 mmol) in 10 ml of 8/1/1 DMSO/H_2O/Pyridine. After 24 h reaction the resulting polymer was dialyzed against deionized water in a 12,000-14,000 MWCO cellulose dialysis membrane. The solvent was removed by lyophilization to yield 190 mg of white solid (yield ~91%).

The average number of PEG groups bound to PGA chains was determined by ^{1}H NMR in $CDCl_3$, comparing the integrated signal at 3.7-3.4 ppm (broad, CH_2 of PEG) with that at 2.4-1.8 ppm

(CH_2 of glutamic acid). The effective degree of modification was found to be 57-60 %. ^{1}H NMR (500 MHz, D_2O) δ: 3.8 (m, br, CH of PGA), 3.7-3.4 (m, br, CH_2 PEG), 2.4-1.8 (m, br, CH_2 of PGA).

Synthesis of PGA-DSPE(10%)-mPEG(60%, 5KDa) (3). PEG-γPGA (60% PEG) (50 mg, 0.0159 mmol) was reacted with 1,2-distearoyl-*sn*-glycero-3-phosphoethanolamine (DSPE) (3.56 mg, 0.0048 mmol) in the presence of 1-ethyl-3-(3-dimethylaminopropyl)carbodiimide hydrochloride (15.2 mg, 0.0795 mmol) (EDC.HCl) in 15mL DMF/NEt_3/$CHCl_3$ 1/1/8. After 24 h reaction the solvent was removed and the resulting polymer was purified to remove byproduct by dialysis with 12,000-14,000 MWCO cellulose dialysis membrane. The solvent was removed by lyophilization to yield 47 mg of (**3**) as white solid (yield~90%).

Estimation of the PEG functionalization and DSPE groups were determined by comparing the integrated signal at 3.4-3.7 ppm (CH_2 of PEG) with that at 2.6-1.8 ppm (CH_2 of PGA) and 1.2-1.4 ppm (CH_2 of DSPE). The effective degree of modification was found to be 9-10 % of DSPE and 57-60% of PGA. ^{1}H NMR (500 MHz, $CDCl_3$) δ: 4.45 and 4.15 and 3.95 (m, br, OCH2 of DSPE), 3.8 (m, br, CH of PGA), 3.7-3.4 (m, br, CH_2 of mPEG), 2.30 (m, br, CH_2 of DSPE) 2.2-1.8 (m, CH_2 of PGA), 1.60 (m, br, CH_2 of DSPE) 1.2-1.4 (CH_2 of DSPE), 0.88 ppm (CH_3 of DSPE).

SWNTs functionalization. Raw Hipco SWNTs (0.20 mg/ml) were sonicated in 4 mL of water solution with (**1**) (3 mg/mL) or (**2**) and (**3**) (4 mg/mL) for 1 h with a bath sonicator, followed by centrifugation at 24,000 g for 6h, yielding a suspension of SWNTs with non-covalent polymer coating. Excess of (**1**), (**2**), or (**3**) was removed by repeated filtration through a polycarbonate membrane (0.2 μm) and extensive washing with water.

Au NPs functionalization with (2) or (3). 2 ml of gold colloid, 20 nm nanoparticles, were sonicated with (**2**) or (**3**) (2 mg/mL) for 15 min with a bath sonicator, yielding a suspension of NPs with

non-covalent γPGA-polymer coating. After 15 min sonication, the resulting NPs were purified in order to remove the original nanoparticle capping ligand (citrate) via dialysis with 12,000-14,000 MWCO. Excess γPGA-polymer was removed by repeated centrifugation at 24,000 g for 10 minutes and re-suspension with water.

Au NPs suspension with thiol-mPEG(5KDa): 2 ml gold colloid 20 nm nanoparticles (from Sigma-Aldrich) were sonicated with thiol-mPEG(5KDa) 3 mg/mL for 15 min with a bath sonicator followed by dialysis, yielding a suspension of NPs with covalent PEG coating. After 15 min sonication, the resulting NPs ware purified to remove the original citrate capping molecules by dialysis with 3,500 MWCO cellulose dialysis membrane. Excess thiol-PEG was removed by repeated centrifugation at 24,000 g for 15 minutes and washing with water.

The NPs-thiol-mPEG(5KDa) are stable only in the presence of excess thiol-mPEG. Indeed, if excess thiol-mPEG is removed by centrifugation, the NP solution becomes unstable and forms agreggates (indicated by a purple solution).

Gold nanorods synthesis: Gold nanorods (Au NRs) were synthesized following by the seeded growth method detailed by Nikoobakht et al[1]. Briefly, a seed solution of gold nanoparticles was formed by adding 5mL of 0.2M cetyltrimethylammonium bromide (CTAB) to 5mL of 0.5 mM $HAuCl_4$. To this solution 0.60 mL of 10 mM freshly prepared, ice-cold $NaBH_4$ was added. The solution was mixed vigorously by sonication for 2 minutes. The growth solution was prepared by mixing 0.25 mL of $AgNO_3$ with 5mL of 0.20 M CTAB, followed by the addition of 5 mL of 1 mM $HAuCl_4$ and gentle mixing. The gold was then reduced by adding 70 μL of 78.8 mM ascorbic acid and the rod-forming reaction was initiated by adding 12 μL of the seed solution to the growth solution at 27-30 ºC. The reaction was completed within 60 minutes.

Au NRs suspension with (2). 2 ml of gold nanorods in CTAB were sonicated with (**2**) (3mg/mL) for 15 min with a bath sonicator, followed by dialysis, yielding a suspension of NPs with non-covalent (**2**) coating. After 15 min sonication, the resulting NRs were purified to remove the original CTAB capping molecules by dialysis with 12,000-14,000 MWCO cellulose dialysis membrane. Excess (**2**) was removed by repeated centrifugation at 24,000 g for 10 minutes and wash with water.

Au NRs suspension with thiol-mPEG(5KDa): Gold nanorods with CTAB were sonicated in a solution of thiol-mPEG(5KDa) for 15 min with a bath sonicator followed by dialysis, yielding a suspension of NRs with covalent thiol-mPEG coating. After 15 min sonication, the resulting NRs were purified to remove the CTAB by dialysis with a 3,500 MWCO membrane. Excess of thiol-mPEG was removed by repeated centrifugation at 24,000 g for 10 minutes and re-suspension with water.

SWNTs Blood circulation test in mice. Six week old balb/c mice were used in our study. Two hundred μL of ~0.1 mg/mL saline solution was intravenously (i.v.) injected into the tail vein of each mouse. Prior to injection of the SWNT solution, a Raman spectrum was recorded and used to calculate the SWNTs concentration based on the calibration curve. At various time points post injection (p.i.), ~5 μL of blood was collected from the tail vein and weighed for accuracy (using a different vein from the injected one) and dissolved in 10 μL of lysis buffer (1% SDS, 1% Triton X-100, 40 mM Tris Acetate, 10 mM EDTA, 10 mM DTT) for detecting SWNTs in the blood by Raman measurement as reported previously[2]. The Raman G band peak areas were measured to calculate the SWNTs concentrations in the blood. The percent injected dose per gram (%ID/g) of blood was calculated by the following equation:

$$\%ID/g = \frac{[SWNT]_{\text{blood lysate}} \times V_{\text{blood lysate}}}{[SWNT]_{\text{injected}} \times V_{\text{injected SWNT}} \times \text{blood weight}} \times 100\%$$

Reference

[1] B. Nikoobakht, M. A. El-Sayed, *Chemistry of Materials* **2003**, *15*, 1957.
[2] Z. Liu, C. Davis, W. B. Cai, L. He, X. Y. Chen, H. J. Dai, *Proceedings of the National Academy of Sciences of the United States of America* **2008**, *105*, 1410.
[3] D. Wang, W. X. Ji, Z. C. Li, L. W. Chen, *Journal of the American Chemical Society* **2006**, *128*, 6556.
[4] N. Nakayama-Ratchford, S. Bangsaruntip, X. M. Sun, K. Welsher, H. J. Dai, *Journal of the American Chemical Society* **2007**, *129*, 2448.
[5] C. S. Thaxton, D. G. Georganopoulou, C. A. Mirkin, *Clinica Chimica Acta* **2006**, *363*, 120.
[6] B. I. Ipe, K. G. Thomas, *Journal of Physical Chemistry B* **2004**, *108*, 13265.
[7] Z. Liu, X. M. Sun, N. Nakayama-Ratchford, H. J. Dai, *Acs Nano* **2007**, *1*, 50.